Chemical Geology 455 (2017) 376–384

Contents lists available at ScienceDirect

Chemical Geology

journal homepage: www.elsevier.com/locate/chemgeo

Different types of liquid immiscibility in carbonatite magmas: A case study of the Oldoinyo Lengai 1993 lava and melt inclusions

Naomi J. Potter [a,*], Vadim S. Kamenetsky [a], Antonio Simonetti [b], Karsten Goemann [c]

[a] School of Physical Sciences, University of Tasmania, Tasmania 7001, Australia
[b] Department of Civil and Environmental Engineering and Earth Sciences, University of Notre Dame, IN 46556, USA
[c] Central Science Laboratory, University of Tasmania, Tasmania 7001, Australia

ARTICLE INFO

Article history:
Received 31 May 2016
Received in revised form 13 September 2016
Accepted 26 September 2016
Available online 28 September 2016

Keywords:
Natrocarbonatite
Carbonatite
Oldoinyo Lengai
Melt inclusions
Liquid immiscibility

ABSTRACT

Oldoinyo Lengai is situated within the Gregory Rift Valley (northern Tanzania) and is the only active volcano erupting natrocarbonatite lava. This study investigates the texture and mineralogy of the June 1993 lava at Oldoinyo Lengai, and presents petrographic evidence of liquid immiscibility between silicate, carbonate, chloride, and fluoride melt phases. The 1993 lava is a porphyritic natrocarbonatite consisting of abundant phenocrysts of alkali carbonates, nyerereite and gregoryite, set in a quenched groundmass, composed of sodium carbonate, khanneshite, Na-sylvite and K-halite, and a calcium fluoride phase. Dispersed in the lava are silicate spheroids (<2 mm) with a cryptocrystalline silicate mineral assemblage wrapped around a core mineral. We have identified several textural features preserved in the silicate spheroids, melt inclusions, and carbonatite groundmass that exhibit evidence of silicate-carbonate, carbonate-carbonate and carbonate-halide immiscibility. Rapid quenching of the lava facilitated the preservation of the end products of these liquid immiscibility processes within the groundmass. Textural evidence (at both macro- and micro-scales) indicates that the silicate, carbonate, chloride and fluoride phases of the lava unmixed at different stages of evolution in the magmatic system.
© 2016 Elsevier B.V. All rights reserved.

1. Introduction

The petrogenetic evolution of silicate magmas is well known and extensively studied due to the preponderance of siliceous-type volcanism worldwide. In contrast, carbonate magmas are rarely observed in nature with the majority identified in intrusive settings and commonly altered post emplacement (Mitchell, 2005; Woolley, 2003). Oldoinyo Lengai (Tanzania) is the sole active volcano that erupts carbonatites and provides an unprecedented opportunity to better understand the magmatic evolution of this non-silicate type of Earth's magmatism.

The most commonly accepted mechanism proposed for the formation of natrocarbonatites is silicate-carbonate liquid immiscibility (Church and Jones, 1995; Dawson et al., 1996; Keller and Krafft, 1990; Kjarsgaard et al., 1995; Mitchell, 2009; Mitchell and Dawson, 2012; Peterson, 1990; Sharygin et al., 2012). Liquid immiscibility is defined as "*the coexistence of two or more liquid phases in equilibrium…[and]…occurs when the sum of the free energies of two melts in less than that of a mixture of them*" Freestone (1989). The rarity of and difficulty in capturing definitive evidence of liquid immiscibility within magmas has posed a challenge for researchers, as the rocks undergo crystallisation and post-magmatic alteration. For evidence to be preserved of the unmixing process, the liquids must either spatially separate or undergo no magmatic or weathering processes after unmixing. Consequently, the process of liquid immiscibility and its role in magmatic differentiation has been largely overlooked.

Melt inclusion and experimental studies are the primary methods used to support the identification of liquid immiscibility during the formation of magmatic rocks. Melt inclusions provide 'snapshots' of melts and fluids at the time of crystallisation and have recorded occurrences of liquid immiscibility in magmas from a variety of different tectonic settings (Kamenetsky and Kamenetsky, 2010; Mitchell, 2009; Panina and Motorina, 2008; Sekisova et al., 2015; Thompson et al., 2007). Experimental work endeavors to reproduce the sequence and composition of the phases appearing in natural rocks, offering theoretical conditions for these unmixing processes (Brooker and Kjarsgaard, 2011; Freestone and Hamilton, 1980; Kjarsgaard and Peterson, 1991; Moore, 2012; Veksler et al., 2012; Wyllie et al., 1990). The small size (<25 μm) and disequilibrium state within the melt inclusions, and the limited applicability of experimental studies to the natural environment renders some of the evidence and interpretations controversial.

Here we describe the texture and mineralogy of natrocarbonatite lava samples from the 1993 eruption at Oldoinyo Lengai and present both petrographic and melt inclusion evidence for the occurrence of liquid immiscibility between silicate, carbonate, chloride, and fluoride melt phases.

* Corresponding author.
E-mail address: pottern@utas.edu.au (N.J. Potter).

http://dx.doi.org/10.1016/j.chemgeo.2016.09.034
0009-2541/© 2016 Elsevier B.V. All rights reserved.

2. Geological setting and previous work

Oldoinyo Lengai, the only active natrocarbonatite volcano in the world, is situated within the Gregory Rift Valley in northern Tanzania. Between June 14 and June 25, 1993, two of the most volumetrically largest lava flows erupted at Oldoinyo Lengai: the massive southern flow and the Chaos Crags flow (Dawson et al., 1994). These eruptions terminated a 10-year period that was dominated by the extrusion of low-volume, highly mobile carbonatite flows (Dawson et al., 1996). The samples investigated here are from the Chaos Crags flow, which is a particularly crystal-rich lava (79–91% by volume), with a similar viscosity to rhyolite (Dawson et al., 1994). Several previous studies have investigated samples from the June 1993 lava and reported detailed descriptions of the eruption with petrography and mineralogy of the lava (Church and Jones, 1995; Dawson et al., 1994; Dawson et al., 1996) and geochemical data (Simonetti et al., 1997).

3. Methodology

The samples were mounted in epoxy resin and polished using kerosene to prevent destruction of soluble minerals and melt inclusions. After exposure, samples were stored in a desiccator to minimise interaction with atmospheric moisture. All analytical work was performed at the Central Science Laboratory (CSL), University of Tasmania, Australia.

Mineral and melt inclusion compositions were determined by backscattered electron (BSE) imaging and energy dispersive X-ray spectrometry (EDS) using a Hitachi SU-70 field emission scanning electron microscope (SEM). Silicate and fluorapatite kernels were analysed using a Cameca SX100 electron microprobe equipped with a tungsten filament and five wavelength dispersive spectrometers (WDS) using 15 kV accelerating voltage, 30 and 20 nA beam current and a 5 and 20 μm beam diameter, respectively. Additional details are provided in Supplementary Methods. Electron backscattered diffraction (EBSD) on a Hitachi SU-70 SEM was used to evaluate the crystallographic orientation of the crystal microstructures. Ion-polishing for EBSD studies was done in Adelaide Microscopy. The EBSD analysis was performed using 20 kV acceleration voltage, around 3 nA beam current and an Oxford AZtec NordlysNano EBSD detector integrated with the EDS system.

4. Results

The lava is a porphyritic natrocarbonatite composed of abundant euhedral to subhedral phenocrysts of alkali carbonates, nyerereite $Na_2Ca(CO_3)_2$ and gregoryite $(Na_2K_2Ca)CO_3$, surrounded by a quenched carbonatite groundmass (Fig. 1). Dispersed in the lava samples are silicate spheroids (<2 mm) characterised by a core kernel (>200 μm) enveloped in a cryptocrystalline assemblage composed of various silicate minerals. The lava has a low to moderate vesicularity (7–26% vesicles), with a size distribution from <50 μm to 10 mm. Small vesicles have subspherical shapes, whereas the large vesicles are irregular and elongated, often showing signs of coalescence.

4.1. Groundmass

The carbonatite groundmass accounts for around 20% of the lavas' volume (excluding vesicles) and is mainly composed of sodium carbonate, khanneshite $(NaCa)_3(Ba,Sr,Ce,Ca)_3(CO_3)_5$, salt aggregates and a CaF phase (Fig. 2). Scattered throughout the carbonatite groundmass are anhedral to subhedral crystals (<20 μm) of apatite, cuspidine $Ca_4(Si_2O_7)(F,OH)_2$, nepheline $(Na,K)AlSiO_4$ and sulphides.

The primary constituent of the groundmass is a sodium-rich carbonate phase (Figs. 2, 3) that has a similar chemical composition to the gregoryite phenocrysts but contains slightly more Na (32% and 31%, respectively) and less Ca (5% and 7%, respectively). Another groundmass carbonate is Ba-rich (38–41 wt.% BaO), similar to khanneshite, distributed sporadically in the lava and has irregular, angular shapes (Fig. 1b). The salt aggregates are composed of two chloride end-members: potassium and sodium chloride, with both phases containing minor Na and K, respectively. Potassium chloride (Na-sylvite) is the primary component with sodium chloride (K-halite) dispersed inside, although there are areas composed of pure halite. Irrespective of their composition, all salt aggregates have spherical to irregular shapes (Fig. 3). The CaF phase exhibits linear, globular, symplectic, and graphic textures (Fig. 3), similar textures have been observed by Church and Jones (1995) and Dawson et al. (1996). The texture of the CaF phase varies throughout the samples and appears to be dependent on the surrounding phases, the most prevalent is the linear intergrowth texture (Fig. 3b). There are several crystallographic orientations observed for a given CaF phase (Fig. 4c; d). The variation in colour in Fig. 4c and d indicates a difference in the orientation of the crystals, that is attributed to changes in the x, y and z axis. The stoichiometric composition is 44–47 wt.% F, 50–53 wt.% Ca and 1–4 wt.% Sr.

The sulphide minerals identified within the groundmass are pyrrhotite, Fe-alabandite MnS, Mn-sphalerite (Zn,Fe)S, djerfisherite $K_6Na(Fe,Cu,Ni)_{22}S_{26}Cl$ and galena. These sulphides mostly occur as small individual (<20 μm) anhedral crystals, as well as rare clusters (25–75 μm). The K-Fe-sulphide mineral has been identified as djerfisherite by the K:Fe:S ratio, despite the lack of Cu, Ni and Cl. The djerfisherite crystals occur as anhedral grains ranging in size from 5 μm to 100 μm, and contain 8–11% K and 38–44% Fe. K-Fe-sulphide minerals have been observed in other natrocarbonatite lavas at Oldoinyo Lengai (Dawson et al., 1995; Jago and Gittins, 1999; Mitchell, 1997; Mitchell, 2006). The irregular distribution of the sulphide minerals throughout the groundmass and in phenocrysts suggests that they were present in the magma prior to eruption, as supported by Mitchell (1997) in the case of the 1995 eruption.

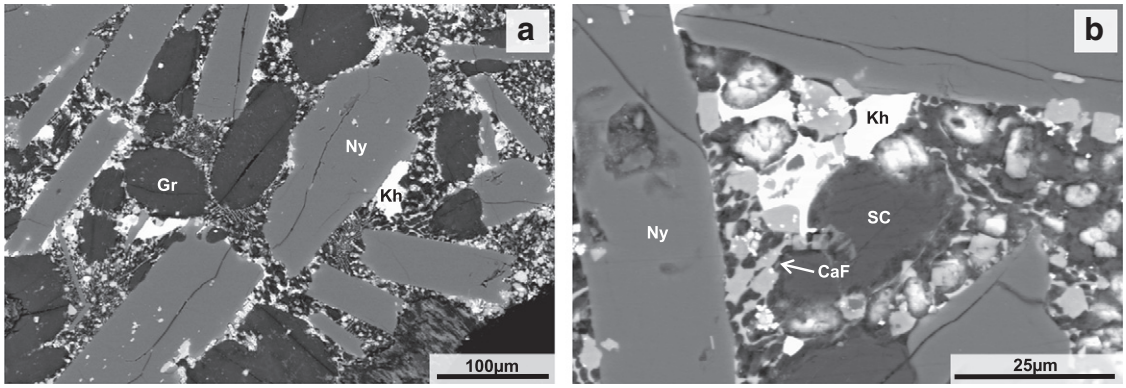

Fig. 1. (a) Back scattered electron (BSE) image of the 1993 lava, with nyerereite and gregoryite phenocrysts surrounded by the carbonatite groundmass. (b) BSE image of khanneshite in the carbonatite groundmass. Abbreviations: CaF – calcium fluoride, Gr – gregoryite, Kh – khanneshite, Ny – nyerereite, SC – sodium carbonate.

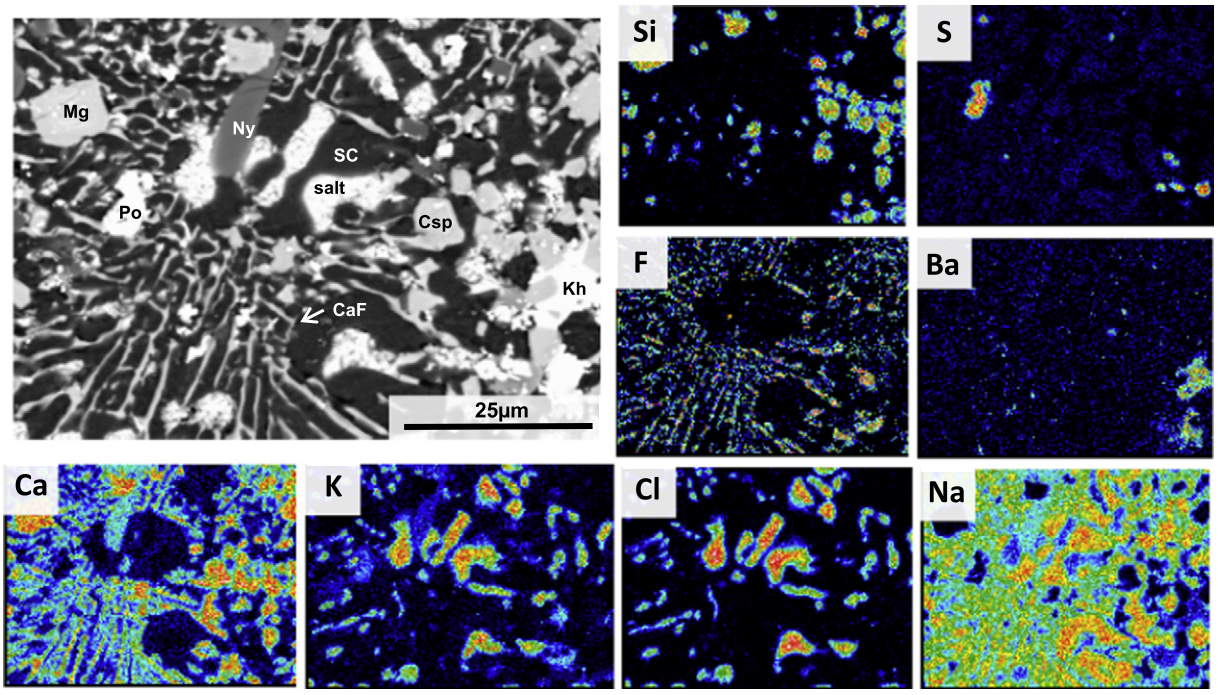

Fig. 2. BSE image and EDS element maps of the carbonatite groundmass. Abbreviations: CaF – calcium fluoride, Csp – cuspidine, Kh – khanneshite, Mg – magnetite, Ny – nyerereite, Po – pyrrhotite, salt – K-halite and Na-sylvite, SC – sodium carbonate.

Other accessory minerals found in the groundmass are euhedral to subhedral crystals of fluorapatite, nepheline, cuspidine, and magnetite with an elevated concentration of Mn (1–4 wt.%). The cuspidine crystals (<20 μm) exhibit oscillatory zoning and contain numerous inclusions of Mn-magnetite. Other rare minerals include a potentially water-bearing potassium sulphate (<10 um) and an unknown Ba-K-Na-Mg fluoride mineral that forms small (<10 μm) anhedral grains. A similar fluoride mineral was identified by Mitchell (1997) as an intermediate member between neighborite and its potassium analogue, identified as K-neighborite (Na,K)MgF_3.

4.2. Silicate spheroids

The silicate spheroids (<2 mm) feature a central kernel (<1 mm) surrounded by a cryptocrystalline assemblage of clinopyroxene, garnet, nepheline, wollastonite, fluorapatite, magnetite, cuspidine and various sulphides (<20 μm; Fig. 5). There is a distinct boundary between the spheroids and the surrounding carbonatite groundmass, with nyerereite phenocrysts oriented around the spheroids (Fig. 5a). The amount of the silicate material around kernels varies from a thin coating (Fig. 5d) to a much greater thickness that can fluctuate around the kernel (Fig. 5a, c). The kernel is usually a single euhedral crystal, or less commonly two or more crystal species either isolated or as a crystal aggregate (Fig. 5a-d). These grains are typically nepheline, clinopyroxene, garnet, wollastonite and fluorapatite. A subspherical carbonate phase is present within the silicate mineral assemblage, ranging in size from 10 to 150 μm (Fig. 5e, f). Some have separated into two carbonate compositions, a Na-rich phase (30–40 wt.% Na_2O), and a Ca-rich phase (23–28 wt.% CaO, 7–8 wt.% K_2O), both have irregular shapes, usually with the Ca-rich phase enveloped by the Na-rich phase.

4.2.1. Kernels

The majority of the nepheline grains have a homogeneous composition (Fig. 5b) with a small number exhibiting minor zonation with antithetic variations in FeO and K_2O concentrations (0.9–2.4 wt.% and 6–7.3 wt.%, respectively). The wollastonite grains are lath-shaped and have homogeneous compositions. Garnet grains belong to the andradite-schorlomite solid solution series and are identified as schorlomite end-members due to their high TiO_2 contents (10–15 wt.%; Fig. 5c). This mineral is referred to as Ti-andrandite by Dawson et al. (1996) and melanite by Church and Jones (1995). Clinopyroxene grains have predominantly low-Al, low-Ti compositions and display irregular oscillatory zoning with varying Mg and Fe contents that are readily observed in the BSE images (higher and lower Mg/Fe ratios correspond to darker and lighter areas, respectively; Fig. 5d). The fluorapatite grains have high F contents (2–3 wt.%) and are less common than the previously mentioned silicate minerals. All kernels contain inclusions (10–50 μm) of other minerals including wollastonite, schorlomite, nepheline, clinopyroxene, titanite, and pyrrhotite. The chemical compositions of the kernels are provided in Supplementary Table S1. Detailed descriptions of the kernels in the silicate spheroids are given in Church and Jones (1995), Dawson et al. (1994) and Dawson et al. (1996).

4.3. Alkali carbonate phenocrysts

The nyerereite phenocrysts are primarily euhedral lath-shaped crystals (Fig. 1) with homogeneous compositions and inclusions (<50 μm) of fluorapatite, unknown Ba-K-Na-Mg fluoride, and small clusters (<50 μm) of cuspidine and djerfisherite crystals (<10 μm). The gregoryite phenocrysts have mostly rounded shapes with no well-defined crystal faces (Fig. 1) and occasionally contain inclusions (5–20 μm) of nyerereite, magnetite and djerfisherite. These crystals differ in their degree of chemical and textural alteration, some phenocrysts have homogenous compositions, while others have perthitic textures with variation in the Na and K content across each phenocryst (4–39 wt.% and 14–33 wt.%, respectively). Some altered phenocrysts display simple lamellar textures, whereas irregular, patchy textures with disseminated halite or K-halite are dominant (Supplementary Figs. S35–40). The lamellar textures suggest the breakdown of the gregoryite solid solution (Dawson et al., 1995). Also, the rims of the chemically altered gregoryite phenocrysts are more texturally uneven than the homogeneous phenocrysts.

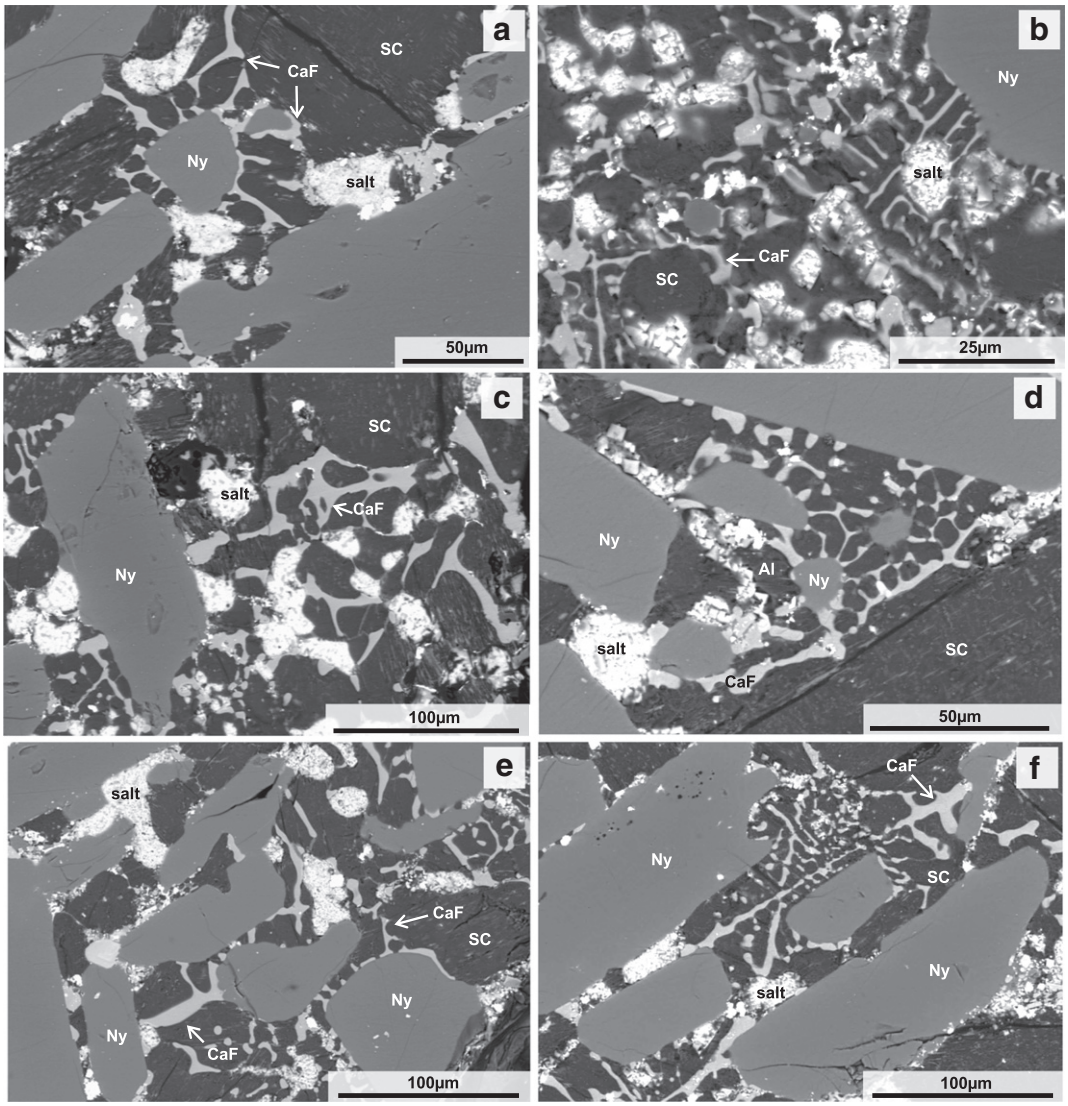

Fig. 3. BSE images of groundmass textures in the June 1993 lava. Abbreviations: Al – Fe-alabandite, CaF – calcium fluoride phase, Ny – nyerereite, salt – K-halite and Na-sylvite, SC – sodium carbonate.

The chemical compositions of the nyerereite and gregoryite phenocrysts do not differ significantly from those documented in other natrocarbonatite lavas, except for the nyerereite phenocrysts which have high BaO contents (up to 3 wt.%; Supplementary Table S2). More details on the composition and textures of nyerereite and gregoryite phenocrysts from other eruptions are described in Mitchell and Kamenetsky (2012), Peterson (1990) and Zaitsev et al. (2009).

4.4. Melt inclusions

The exposed silicate and carbonate melt inclusions have a negative crystallographic shape and are randomly distributed throughout the crystals (Fig. 6). These are primary melt inclusions and represent the melt composition at the time of entrapment, but may not represent the bulk composition as all phases may not have been observed.

4.4.1. Silicate spheroids

The silicate melt inclusions (10 to 50 μm) are identified in all the silicate kernel minerals (nepheline, wollastonite, clinopyroxene and schorlomite; Fig. 6a-e). The glasses are silica-undersaturated and highly enriched in alkali elements (Supplementary Table S3). The majority of the silicate melt inclusions contain small Na-rich carbonate globules (2–10 μm) and occasionally enclose small crystals (2–5 μm) of apatite, clinopyroxene, magnetite and pyrrhotite. The wollastonite-hosted melt inclusions are also characterised by the presence of annite (10 to 30 vol.%; Fig. 6c).

The clinopyroxene and schorlomite phenocrysts contain both silicate and silicate-carbonate melt inclusions. The silicate-carbonate melt inclusions contain Na-rich carbonate globules along with a polycrystalline carbonate globule (5–20 μm) composed of a fine-grained aggregate of Na-rich and Ca-rich carbonate phases, similar to the carbonate component in the silicate spheroids (Fig. 6d, e).

4.4.2. Alkali carbonate and fluorapatite phenocrysts

Primary carbonate melt inclusions (5–25 μm) have been identified in nyerereite, gregoryite and fluorapatite phenocrysts (Fig. 6f-i). These melt inclusions are scarce in comparison to the silicate melt inclusions as nyerereite and gregoryite typically lack melt inclusions. The carbonate melt inclusions have comparable chemical compositions to the carbonatite groundmass. The fluorapatite-hosted carbonate melt inclusions contain Na-rich carbonate and inclusions of apatite, magnetite and calcite (Fig. 6f). Some of the melt inclusions have separated into an alkali carbonate and khanneshite, with daughter phases of cuspidine, nepheline, and an unknown Ba-K-Na-Mg fluoride (Fig. 6g). Rare melt

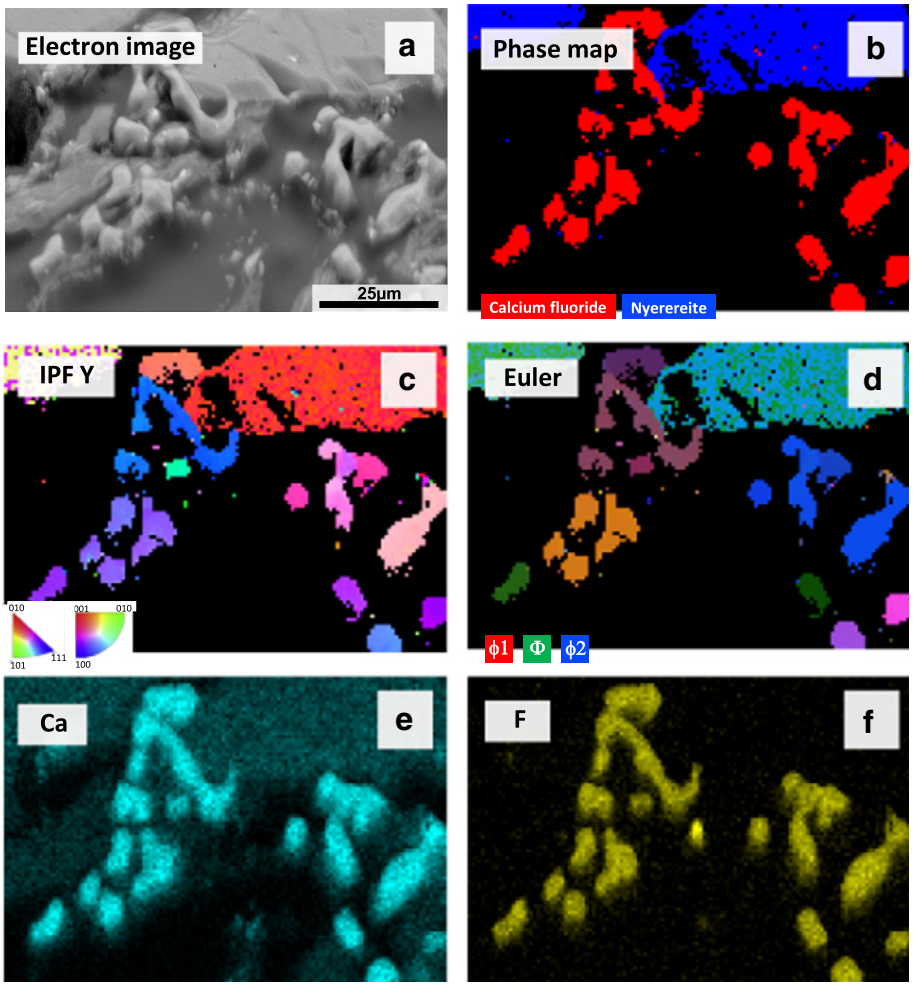

Fig. 4. (a) Electron image of the area mapped with a clear outline of the calcium fluoride (CaF) phase, (b) Phase map based on combined EDS and EBSD data showing the CaF phase, (c) Inverse pole figure (IPF) map in the Y direction showing varying crystal orientations in different colours, (d) Euler angle map using colours to denote the variety of crystal orientations in space using Euler angles: φ1-red φ-green, φ2-blue, (e-f) EDS compositional maps showing the uniform concentration of calcium and fluorine in the CaF phase.

inclusions hosted in gregoryite contain a single nyerereite crystal in a heterogeneous carbonate-Na-sylvite matrix (Fig. 6h). In contrast, the nyerereite phenocrysts contain abundant melt inclusions, composed of sodium carbonate, CaF and Na-sylvite with trapped crystals of cuspidine, apatite, and magnetite (Fig. 6i).

5. Discussion

5.1. Silicate-carbonate immiscibility

Occurrences of silicate-carbonate liquid immiscibility are widespread in nature and have been well documented in several alkaline carbonate-bearing complexes (Guzmics et al., 2011; Guzmics et al., 2012; Lloyd and Stoppa, 2003; Mitchell, 2009; Mitchell and Dawson, 2012; Nielsen et al., 1997; Panina, 2005; Sharygin et al., 2012; Zaitsev et al., 2009). In our study, textural features of the silicate spheroids, melt inclusions and carbonatite groundmass provide evidence of silicate-carbonate immiscibility. The main textural evidence that supports liquid immiscibility in the lava is the distinct boundaries between different compositions in the melt inclusions and groundmass.

As textural evidence for liquid immiscibility is rarely preserved in rocks, melt inclusions are fundamental for the identification of unmixing in natural systems. The onset of silicate-carbonate immiscibility in carbonate-rich magmatic systems is an area of ongoing research, and there have been several heating experiments on synthetic and natural samples to determine the temperature and pressure of unmixing (Freestone and Hamilton, 1980; Kjarsgaard et al., 1995; Koster van Groos and Wyllie, 1966; Sharygin et al., 2012).

The silicate spheroids are identified as immiscible droplets of nephelinitic composition, which is consistent with previous interpretations (Church and Jones, 1995; Dawson et al., 1994; Dawson et al., 1996). The distinct boundary between the spheroids and the surrounding carbonatite, the rounded shape of the spheroids, the orientation of the nyerereite phenocrysts around the spheroids and the absence of penetration by these phenocrysts (Fig. 5a, b), all support the idea that silicate-carbonate liquid immiscibility enabled the formation of the silicate spheroids. These textures also suggest that the silicate spheroids were molten when first enveloped by the carbonate melt, enabling a subspherical shape. The silicate spheroids subsequently cooled and solidified prior to the crystallisation of the surrounding carbonate melt preventing the carbonate melt from penetrating the spheroids, an interpretation first proposed by Dawson et al. (1996).

The presence of the carbonate component within the silicate mineral assemblage in the spheroids (Fig. 5e, f) suggests that silicate-carbonate immiscibility proceeds with changes in temperature and pressure in the magmatic system. The carbonate components have comparable chemical compositions, however, some have separated into Ca-rich and Na-rich phases similar to the carbonate globules in the silicate-carbonate melt inclusions (e.g. Fig. 6d), suggesting that the carbonate melt had a comparable chemical composition during unmixing. Dawson et al.

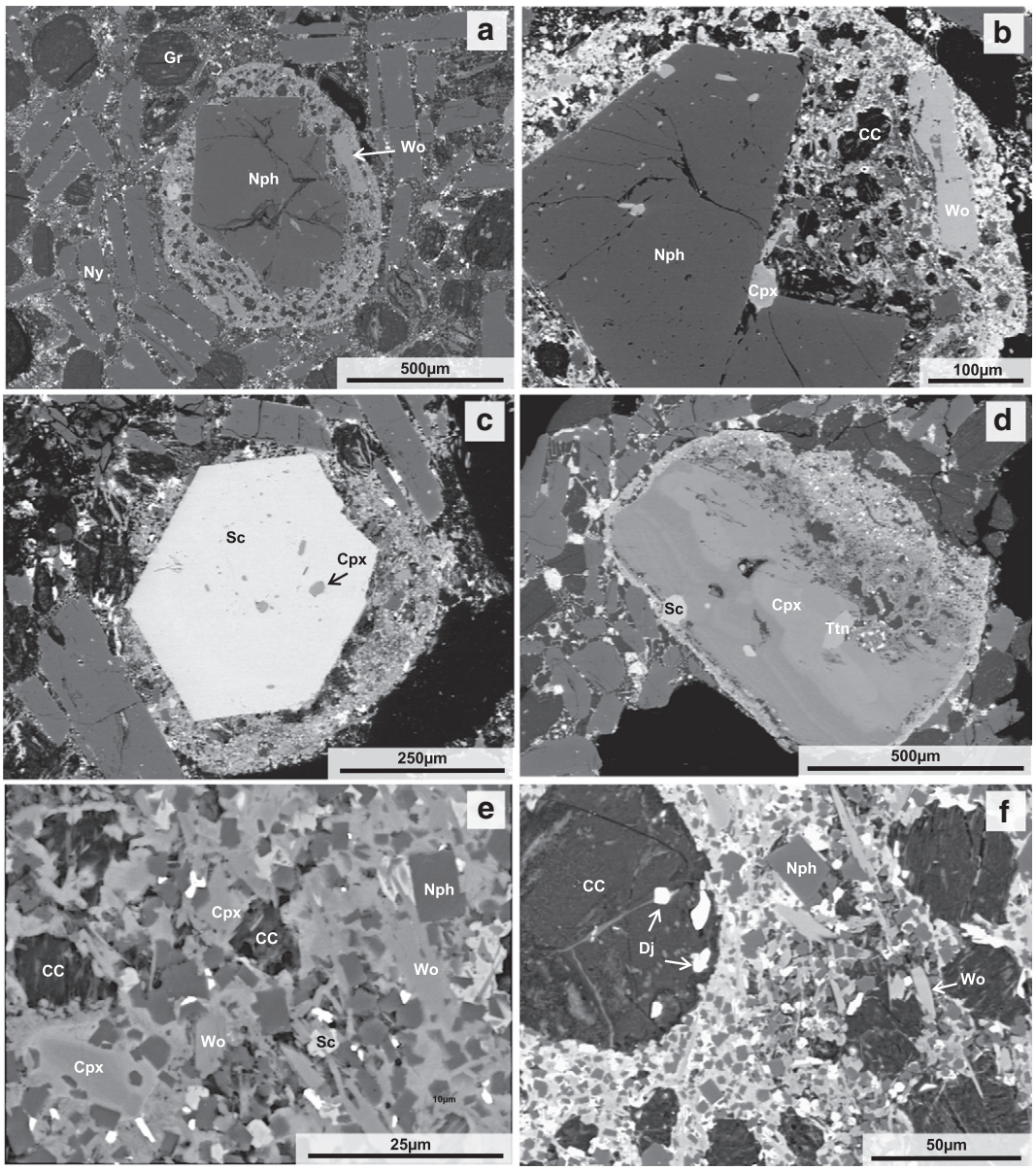

Fig. 5. BSE images of silicate spheroids in the June 1993 lava. (a, b) Nepheline kernel surrounded by a silicate mineral assemblage, (c) Schorlomite kernel surrounded by a silicate mineral assemblage, (d) Clinopyroxene kernel surrounded by a thin coating of the silicate mineral assemblage, (e, f) Close up of the silicate mineral assemblage within the silicate spheroids. Abbreviations: CC – carbonate component, Cpx – clinopyroxene, Dj – djerfisherite, Gr – gregoryite, Nph – nepheline, Ny – nyerereite, Sc – schorlomite, Ttn – titanate, Wo – wollastonite.

(1994) suggested "*the presence of carbonatite phases in the glasses entrapped in both the spheroid silicate phenocrysts and the spheroid matrix indicates that the spheroids are exhibiting multiple episodes of separation of carbonatite from a silicate melt*". The timing of separation of the carbonate component from the surrounding silicate melt remains unknown. However, we suggest that liquid immiscibility during magmatic ascent and cooling could have enabled the separation of the carbonate component from the surrounding silicate melt. Another possiblility could be that the carbonate component was trapped in the silicate melt when the silicate spheroids were first incorporated into the natrocarbonatite magma at the top of the magma chamber.

The kernels in the silicate spheroids do not represent phenocrysts in the natrocarbonatite magma, but they crystallised from the nephelinitic melt in the magma chamber. The kernels host silicate melt inclusions that are interpreted to represent the parental peralkaline nephelinitic magma in the magma chamber. The coexsistence of silicate and silicate-carbonate melt inclusions in the clinopyroxene and schorlomite kernels is the evidence for onset of silicate-carbonate liquid immiscibility, with the separation of the melt into two coexisting silicate and carbonate liquids.

The presence of cuspidine, nepheline and tilleyite in the groundmass is evidence that silica was present in the natrocarbonatite magma during crystallisation (Fig. 2; Dawson et al., 1996). The crystallisation of cuspidine is enabled by the significant concentration of fluorine in the natrocarbonatite magma.

5.1.1. Petrogenesis of silicate spheroids

The presence of silicate spheroids has not been reported in other natrocarbonatite lavas at Oldoinyo Lengai. The petrogenic model envisaged for the formation of these silicate spheroids in the 1993 lava is an adaptation of the processes suggested by Church and Jones (1995), Dawson et al. (1994) and Dawson et al. (1996), and is summarised here (Fig. 7). Prior to the 1993 eruption an injection of peralkaline nephelinitic magma intruded into the magma chamber (Fig. 7b). The intrusion disrupted the carbonate crystal mush at the top of the magma chamber that contains a high modal abundance of nyerereite and

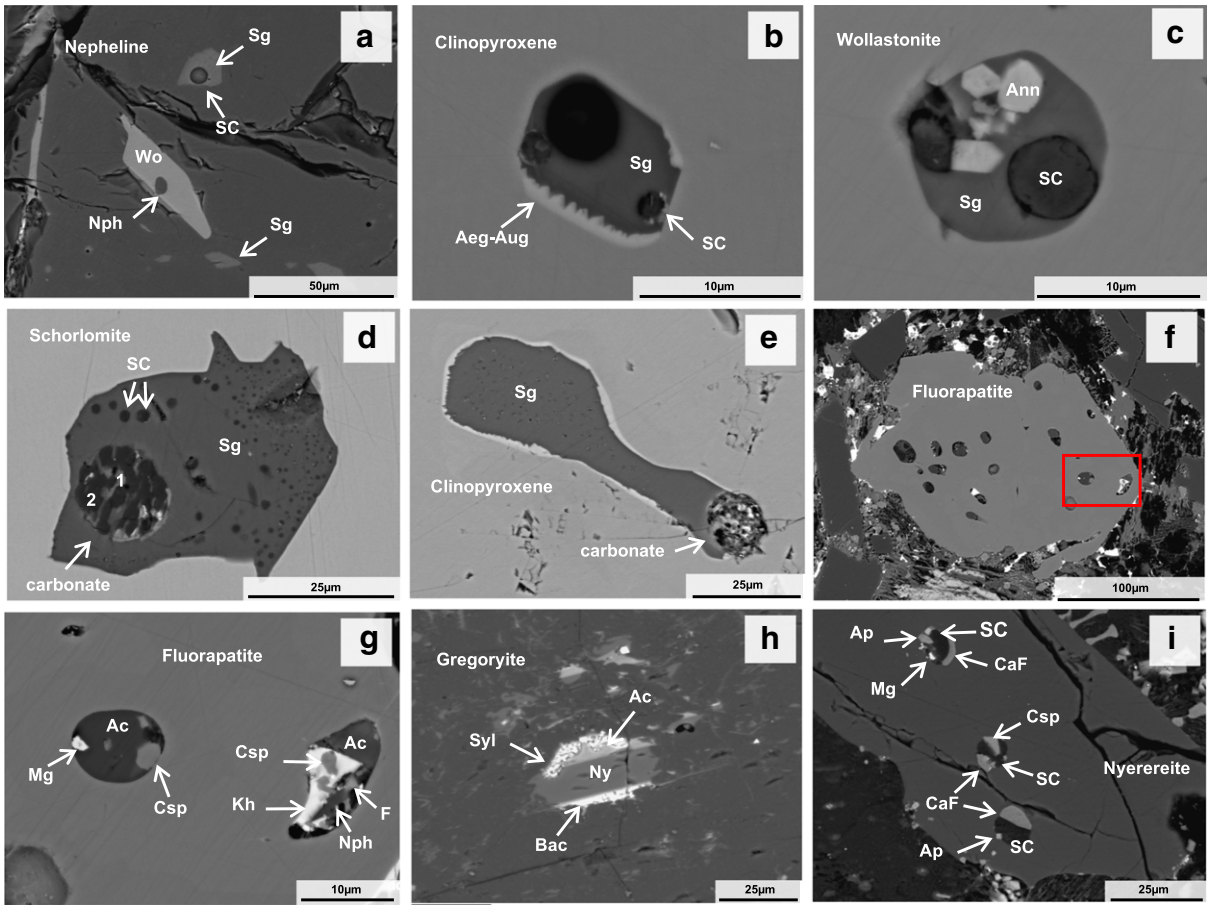

Fig. 6. BSE images of silicate and carbonate melt inclusions. (a) Nepheline kernel with silicate melt inclusions, (b) Clinopyroxene-hosted silicate melt inclusion with an intermediate reaction rim of aegirine-augite, (c) Wollastonite-hosted silicate melt inclusion, (d) Schorlomite-hosted silicate melt inclusion with a carbonate globule, (e) Clinopyroxene-hosted silicate melt inclusion with a carbonate globule, (f) Fluorapatite phenocryst in the carbonatite groundmass with numerous carbonate melt inclusions, (g) A close up of carbonate melt inclusions in the fig. 6f fluorapatite phenocryst, (h) Gregoryite-hosted carbonate melt inclusion, (i) Nyerereite-hosted carbonate melt inclusion. Abbreviations: Ac – alkali-carbonate, Aeg – aegirine, Ann – annite, Ap – apatite, Aug. – augite, Bac – barium-rich carbonate, CaF – calcium fluoride phase, Csp – cuspidine, F – unknown Ba-K-Na-Mg fluoride, Kh – khanneshite, Mg – magnetite, Nph – nepheline, Ny – nyerereite, SC – sodium carbonate, Sg – silicate glass, Syl – Na-sylvite, Wo – wollastonite, 1 – calcium-rich phase, 2 – sodium-rich phase.

gregoryite phenocrysts (Dawson et al., 1994; Dawson et al., 1996). This enabled the incorporation of silicate kernels into the natrocarbonatite magma, with a silicate melt surrounding the kernels (Fig. 7c). The elevated viscosity of the 1993 natrocarbonatite magma (i.e. nyerereite and gregoryite crystal mush; Dawson et al., 1994; Dawson et al., 1996) prevented the silicate spheroids from settling back into the nephelinitic magma (Fig. 7c).

5.2. Carbonate-carbonate immiscibility

Two carbonate phases have been identified within the groundmass of the June 1993 lava: sodium carbonate and khanneshite. Dawson et al. (1996) also identified two carbonate groundmass phases, a gregoryite-like phase and a Ba-rich carbonate phase referred to as witherite. The Ba-rich carbonate phase has a variety of compositions in other natrocarbonatite lavas, most likely caused by the different chemical compositions of the carbonate melt (Dawson et al., 1996; Mitchell, 1997; Mitchell, 2006; Peterson, 1990). The identification of two different carbonate phases in these natrocarbonatite lavas points to unmixing of carbonates as a common feature of lavas at Oldoinyo Lengai.

We suggest that carbonate-carbonate immiscibility occurred during quenching. The separation produced khanneshite and a homogeneous Na-K-rich carbonate phase containing fluorine and chlorine, which subsequently separates into sodium carbonate, CaF, and salt. The immiscible separation of these two carbonate phases was supported by Mitchell (1997), whereas Dawson et al. (1996) attributed the presence of two carbonate phases rather than one homogeneous carbonate phase (Phase X) and the coarser grain size of the "*sylvite and fluorite*" is due to slower cooling of the June 1993 lava.

5.3. Carbonate-halide immiscibility

We interpret the intergrown textures and chemical compositions of the groundmass phases: sodium carbonate, khanneshite, CaF and salt, and the presence of these same phases within the carbonate melt inclusions, to be evidence for carbonate-halide immiscibility in the June 1993 eruption at Oldoinyo Lengai. The presence of multiphase carbonate-halide immiscibility is identified by textural relationships between the carbonate, chloride, and fluoride phases in the groundmass and within the carbonate- and apatite-hosted melt inclusions. The melt inclusions have similar chemical compositions and textures as the carbonatite groundmass, which indicates that the same unmixing processes occurred on both macro- and micro-scales (Figs. 3, 6g-i). Subspherical to irregular shapes of the mixed Na-sylvite and K-halite aggregates are common in the groundmass of natrocarbonatites (Church and Jones, 1995; Dawson et al., 1995; Dawson et al., 1996; Keller and Krafft, 1990; Mitchell, 1997; Mitchell, 2006) and are most likely caused by sporadic unmixing of the chloride liquid (Fig. 3). The CaF phase has been identified in other natrocarbonatite lavas as "*intergrown fluorite with a gregoryite-like mineral*" (Church and Jones, 1995; Dawson et al., 1996; Mitchell, 1997; Mitchell, 2006). The EBSD data shows that the CaF phase has relatively homogeneous crystalline structures (Fig. 4), but

has a distinctive texture that is typical of a liquid occurring interstitially to solid phases (e.g. nyerereite in this case; Fig. 3). The high crystal content of the lava, and thus inferred high degree of crystallisation, could have led to high concentrations of fluorine and chlorine in the residual melt, prompting unmixing of halide liquids on quenching. The process of liquid immiscibility during quenching and related textures are best depicted in experimental works with carbonate-silicate compositions, where the melt components form 'immiscibility' textures, and bona fide crystallographic shapes do not have time to develop (Brooker and Kjarsgaard, 2011; Kamenetsky and Yaxley, 2015). Immiscible carbonate-halide intergrowths have been described in other natrocarbonatite lavas with different proportion and composition of the unmixed components (Mitchell, 1997; Mitchell, 2006; Peterson, 1990). The rapid quenching of the lava facilitated the preservation of the end products of these immiscibility processes within the groundmass.

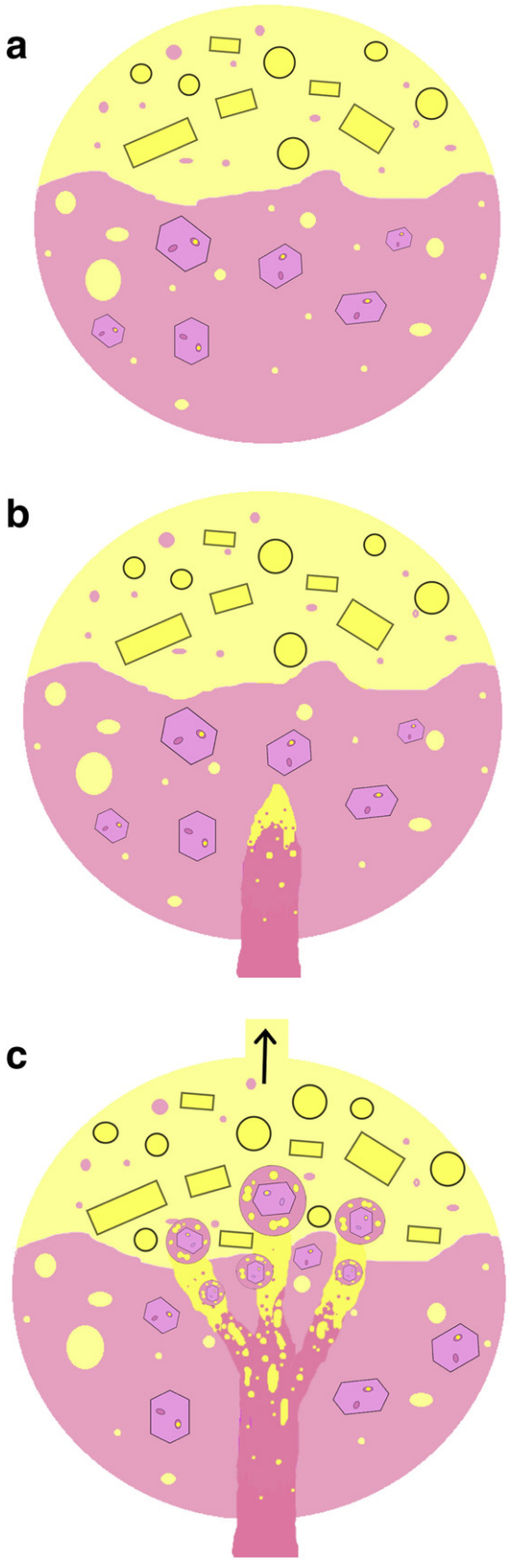

5.4. Multistage immiscibility

The mineralogical and textural features of the studied samples support the following origin of the 1993 natrocarbonatite lava at Oldoinyo Lengai (Fig. 7). The unmixing of the silicate, carbonate, chloride and fluoride components can be separated into different stages of evolution in the magmatic system and represent both high- and low-pressure immiscibility.

The first stage of liquid immiscibility is recorded by the silicate spheroids and the silicate melt inclusions within the central kernels. The observation of sodium carbonate globules and fine-grained carbonate aggregates in the silicate melt inclusions indicates that the onset of silicate-carbonate liquid immiscibility happened prior to the crystallisation of the silicate minerals in the magma chamber. This immiscibility resulted in the spatial separation of the carbonate melt from the parental peralkaline nephelinitic melt in the magma chamber (Fig. 7a; Dawson et al., 1992; Mitchell, 1997; Sharygin et al., 2012). Our interpretations support that the separation happened at a shallow level within the magma plumbing system at Oldoinyo Lengai (Freestone and Hamilton, 1980; Keller and Zaitsev, 2012; Kervyn et al., 2008; Kjarsgaard et al., 1995).

The second stage of immiscibility occurred during eruption, as the decreasing temperature and pressure promotes unmixing in the carbonate melt, generating a heterogeneous mix of four immiscible phases. These fractions are represented by the two carbonate phases: sodium carbonate and khanneshite, and the two halide phases: CaF and Na-sylvite and K-halite salt aggregates.

6. Conclusions

1. The evidence presented suggests that liquid immiscibility occurred between silicate, carbonate, chloride, and fluoride melt phases in the June 1993 natrocarbonatite, and show that multi-stage liquid immiscibility is a major factor in the petrogenesis of this lava at Oldoinyo Lengai.
2. The identification of carbonate-carbonate and carbonate-halide immiscibility within the natrocarbonatite lava shows that different types of liquid immiscibility, other than silicate-silicate and silicate-carbonate, can occur in natural magmas. The identification of these

Fig. 7. (a) Stratified magma chamber with an emulsion of nephelinitic magma overlain by natrocarbonatite magma. The stratification is a result of silicate-carbonate immiscibility. The high modal abundance of gregoryite and nyerereite phenocrysts in the lava indicates that there was a high crystal content in the natrocarbonatite magma prior to eruption, identified as a carbonate crystal mush (Dawson et al., 1994; Dawson et al., 1996). (b) A new injection of nephelinitic magma intrudes into the magma chamber. As the intrusion rises and cools, it undergoes immiscibility and partially separates into carbonate and silicate melts, with the carbonate segregation accumulating at the top of the intrusion. (c) The carbonate head of the intrusion disrupts the carbonate crystal mush at the top of the magma chamber, and pushes silicate minerals into the carbonate crystal mush. The high density of crystals enabled these silicate spheroids to become trapped within the surrounding natrocarbonatite magma (Church and Jones, 1995; Dawson et al., 1994; Dawson et al., 1996). The intrusion of new ascending melt may also cause mixing within the surrounding magma. It cannot be specified whether the silicate spheroids came from the intrusion or the surrounding nephelinitic magma.

diverse unmixed phases at both the macro- and micro-scale presents clear evidence that several types of liquid immiscibility happen during evolution of a single melt, both in the magma plumbing system and during eruption.

3. Liquid immiscibility is rarely observed in the rock record due to masking effects of crystallisation and alteration, but can be observed in melt inclusion and experimental studies. The identification of unmixing in the lavas' groundmass has the potential to provide a new avenue for studying liquid immiscibility in natural magmas.

Acknowledgements

The samples of fresh natrocarbonatite lava from the Chaos Crags lava flow were collected by C. Shardy from the northern (active) crater floor of Oldoinyo Lengai on June 29, 1993. We would like to thank Aoife McFadden at Adelaide Microscopy for ion polishing. We are grateful to Adrian Jones, David Pyle, Matt Ferguson and the two anonymous reviewers for their helpful criticism and suggestions. This research was supported by the Australian Research Council (Discovery Grant DP130100257) to V. Kamenetsky.

Appendix A. Supplementary data

Supplementary data to this article can be found online at http://dx.doi.org/10.1016/j.chemgeo.2016.09.034.

References

Brooker, R.A., Kjarsgaard, B.A., 2011. Silicate-carbonate liquid immiscibility and phase relations in the system SiO_2-Na_2O-Al_2O_3-CaO-CO_2 at 0.1-2.5 GPa with applications to carbonatite genesis. J. Petrol. 52, 1281–1305.

Church, A.A., Jones, A.P., 1995. Silicate-carbonate immiscibility at Oldoinyo Lengai. J. Petrol. 36, 869–889.

Dawson, J.B., Pinkerton, H., Norton, G.E., Pyle, D.M., Browning, P., Jackson, D., Fallick, A.E., 1995. Petrology and geochemistry of Oldoinyo Lengai lavas extruded in November 1988: magma source, ascent and crystallization. In: Bell, K., Keller, J. (Eds.), Carbonatite Volcanism. Springer, pp. 47–69.

Dawson, J.B., Pinkerton, H., Pyle, D.M., Nyamweru, C., 1994. June 1993 eruption of Oldoinyo Lengai, Tanzania: exceptionally viscous and large carbonatite lava flows and evidence for coexisting silicate and carbonate magmas. Geology 22, 799–802.

Dawson, J.B., Pyle, D.M., Pinkerton, H., 1996. Evolution of natrocarbonatite from a wollastonite nephelinite parent: evidence from the June 1993 eruption of Oldoinyo Lengai, Tanzania. J. Geol. 41–54.

Dawson, J.B., Smith, J.V., Steele, I.M., 1992. 1966 ash eruption of the carbonatite volcano Oldoinyo Lengai: mineralogy of lapilli and mixing of silicate and carbonate magmas. Mineral. Mag. 56, 1–16.

Freestone, I.C., 1989. Liquid Immiscibility, Petrology. Springer, pp. 281–283.

Freestone, I.C., Hamilton, D.L., 1980. The role of liquid immiscibility in the genesis of carbonatites - an experimental study. Contrib. Mineral. Petrol. 73, 105–117.

Guzmics, T., Mitchell, R.H., Szabó, C., Berkesi, M., Milke, R., Abart, R., 2011. Carbonatite melt inclusions in coexisting magnetite, apatite and monticellite in Kerimasi calciocarbonatite, Tanzania: melt evolution and petrogenesis. Contrib. Mineral. Petrol. 161, 177–196.

Guzmics, T., Mitchell, R.H., Szabó, C., Berkesi, M., Milke, R., Ratter, K., 2012. Liquid immiscibility between silicate, carbonate and sulfide melts in melt inclusions hosted in co-precipitated minerals from Kerimasi volcano (Tanzania): evolution of carbonated nephelinitic magma. Contrib. Mineral. Petrol. 164, 101–122.

Jago, B.C., Gittins, J., 1999. Mn- and F-bearing rasvumite in natrocarbonatite at Oldoinyo Lengai volcano, Tanzania. Mineral. Mag. 63, 53–55.

Kamenetsky, V.S., Kamenetsky, M.B., 2010. Magmatic fluids immiscible with silicate melts: examples from inclusions in phenocrysts and glasses, and implications for magma evolution and metal transport. Geofluids 10, 293–311.

Kamenetsky, V.S., Yaxley, G.M., 2015. Carbonate–silicate liquid immiscibility in the mantle propels kimberlite magma ascent. Geochim. Cosmochim. Acta 158, 48–56.

Keller, J., Krafft, M., 1990. Effusive natrocarbonatite activity of Oldoinyo Lengai, June 1988. Bull. Volcanol. 52, 629–645.

Keller, J., Zaitsev, A.N., 2012. Geochemistry and petrogenetic significance of natrocarbonatites at Oldoinyo Lengai, Tanzania: Composition of lavas from 1988 to 2007. Lithos 148, 45–53.

Kervyn, M., Ernst, G.G.J., Klaudius, J., Keller, J., Kervyn, F., Mattsson, H.B., Belton, F., Mbede, E., Jacobs, P., 2008. Voluminous lava flows at Oldoinyo Lengai in 2006: chronology of events and insights into the shallow magmatic system. Bull. Volcanol. 70, 1069–1086.

Kjarsgaard, B., Peterson, T., 1991. Nephelinite-carbonatite liquid immiscibility at Shombole volcano, East Africa: petrographic and experimental evidence. Mineral. Petrol. 43, 293–314.

Kjarsgaard, B.A., Hamilton, D.L., Peterson, T.D., 1995. Peralkaline nephelinite/carbonatite liquid immiscibility: comparison of phase compositions in experiments and natural lavas from Oldoinyo Lengai. In: Bell, K., Keller, J. (Eds.), Carbonatite Volcanism. Springer, pp. 163–190.

Koster van Groos, A.F., Wyllie, P.J., 1966. Liquid immiscibility in the system Na_2O-Al_2O_3-SiO_2-CO_2 at pressures up to 1 kilobar. Am. J. Sci. 264, 234–235.

Lloyd, F.E., Stoppa, F., 2003. Pelletal lapilli in diatremes—some inspiration from the old masters. Geolines 15, 65–71.

Mitchell, R.H., 1997. Carbonate-carbonate immiscibility, neighborite and potassium iron sulphide in Oldoinyo Lengai natrocarbonatite. Mineral. Mag. 61, 779–789.

Mitchell, R.H., 2005. Carbonatites and carbonatites and carbonatites. Can. Mineral. 43, 2049–2068.

Mitchell, R.H., 2006. Sylvite and fluorite microcrysts, and fluorite-nyerereite intergrowths from natrocarbonatite, Oldoinyo Lengai, Tanzania. Mineral. Mag. 70, 103–114.

Mitchell, R.H., 2009. Peralkaline nephelinite–natrocarbonatite immiscibility and carbonatite assimilation at Oldoinyo Lengai, Tanzania. Contrib. Mineral. Petrol. 158, 589–598.

Mitchell, R.H., Dawson, J.B., 2012. Carbonate-silicate immiscibility and extremely peralkaline silicate glasses from Nasira cone and recent eruptions at Oldoinyo Lengai volcano, Tanzania. Lithos 152, 40–46.

Mitchell, R.H., Kamenetsky, V.S., 2012. Trace element geochemistry of nyerereite and gregoryite phenocrysts from natrocarbonatite lava, Oldoinyo Lengai, Tanzania: Implications for magma mixing. Lithos 152, 56–65.

Moore, K.R., 2012. Experimental study in the Na_2O–CaO–MgO–Al_2O_3–SiO_2–CO_2 system at 3 GPa: the effect of sodium on mantle melting to carbonate-rich liquids and implications for the petrogenesis of silicocarbonatites. Mineral. Mag. 76, 285–309.

Nielsen, T.F.D., Solovova, I.P., Veksler, I.V., 1997. Parental melts of melilitolite and origin of alkaline carbonatite: evidence from crystallised melt inclusions, Gardiner complex. Contrib. Mineral. Petrol. 126, 331–344.

Panina, L.I., 2005. Multiphase carbonate-salt immiscibility in carbonatite melts: data on melt inclusions from the Krestovskiy massif minerals (Polar Siberia). Contrib. Mineral. Petrol. 150, 19–36.

Panina, L.I., Motorina, I.V., 2008. Liquid immiscibility in deep-seated magmas and the generation of carbonatite melts. Geochem. Int. 46, 448–464.

Peterson, T.D., 1990. Petrology and genesis of natrocarbonatite. Contrib. Mineral. Petrol. 105, 143–155.

Sekisova, V.S., Sharygin, V.V., Zaitsev, A.N., Strekopytov, S., 2015. Liquid immiscibility during crystallization of forsterite-phlogopite ijolites at Oldoinyo Lengai volcano, Tanzania: study of melt inclusions. Russ. Geol. Geophys. 56, 1717–1737.

Sharygin, V.V., Kamenetsky, V.S., Zaitsev, A.N., Kamenetsky, M.B., 2012. Silicate–natrocarbonatite liquid immiscibility in 1917 eruption combeite–wollastonite nephelinite, Oldoinyo Lengai Volcano, Tanzania: Melt inclusion study. Lithos 152, 23–39.

Simonetti, A., Bell, K., Shrady, C., 1997. Trace-and rare-earth-element geochemistry of the June 1993 natrocarbonatite lavas, Oldoinyo Lengai (Tanzania): Implications for the origin of carbonatite magmas. J. Volcanol. Geotherm. Res. 75, 89–106.

Thompson, A.B., Aerts, M., Hack, A.C., 2007. Liquid immiscibility in silicate melts and related systems. Rev. Mineral. Geochem. 65, 99–127.

Veksler, I.V., Dorfman, A.M., Dulski, P., Kamenetsky, V.S., Danyushevsky, L.V., Jeffries, T., Dingwell, D.B., 2012. Partitioning of elements between silicate melt and immiscible fluoride, chloride, carbonate, phosphate and sulfate melts, with implications to the origin of natrocarbonatite. Geochim. Cosmochim. Acta 79, 20–40.

Woolley, A.R., 2003. Igneous silicate rocks associated with carbonatites: their diversity, relative abundances and implications for carbonatite genesis. Periodico di Mineralogia 72, 17.

Wyllie, P.J., Baker, M.B., White, B.S., 1990. Experimental boundaries for the origin and evolution of carbonatites. Lithos 26, 3–19.

Zaitsev, A.N., Keller, J., Spratt, J., Jeffries, T.E., Sharygin, V.V., 2009. Chemical composition of nyerereite and gregoryite from natrocarbonatites of Oldoinyo Lengai volcano, Tanzania. Geol. Ore Deposits 51, 608–616.